arXiv:2504.14860v1 [cs.CV] 21 Apr 2025

Bridge the Gap: From Weak to Full Supervision for Temporal Action Localization with PseudoFormer

Ziyi Liu
University of Science and Technology Beijing
liuziyi.iair@gmail.com

Yangcen Liu
Georgia Institute of Technology
yliu3735@gatech.edu

Abstract

Weakly-supervised Temporal Action Localization (WTAL) has achieved notable success but still suffers from a lack of temporal annotations, leading to a performance and framework gap compared with fully-supervised methods. While recent approaches employ pseudo labels for training, three key challenges: generating high-quality pseudo labels, making full use of different priors, and optimizing training methods with noisy labels remain unresolved. Due to these perspectives, we propose ***PseudoFormer****, a novel two-branch framework that bridges the gap between weakly and fully-supervised Temporal Action Localization (TAL). We first introduce RickerFusion, which maps all predicted action proposals to a global shared space to generate pseudo labels with better quality. Subsequently, we leverage both snippet-level and proposal-level labels with different priors from the weak branch to train the regression-based model in the full branch. Finally, the uncertainty mask and iterative refinement mechanism are applied for training with noisy pseudo labels. PseudoFormer achieves state-of-the-art WTAL results on the two commonly used benchmarks, THUMOS14 and ActivityNet1.3. Besides, extensive ablation studies demonstrate the contribution of each component of our method.*

1. Introduction

Weakly-supervised Temporal Action Localization (WTAL), which aims to use video-level annotations to identify and localize temporal action instance, has gained significant traction in recent years [9, 21, 29, 36, 48]. Despite the progress, a substantial gap remains between weakly-supervised and fully-supervised TAL methods, in both the framework and performance. WTAL methods predominantly rely on Multiple Instance Learning (MIL) [30] for localization-by-classification, while TAL approaches often employ regression models to learn from densely annotated proposals. Although recent work [33] has explored using regression models to learn from generated labels, a more comprehensive approach to effectively bridge the gap of framework and performance between WTAL and TAL remains an open challenge.

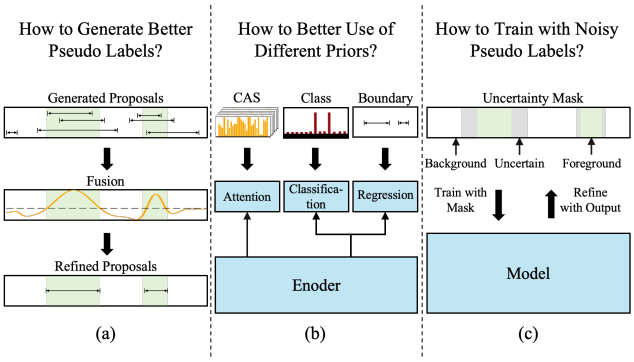

Figure 1. Our paper aims at addressing the three primary questions: (a) How to improve the quality of generated labels from the base model? (b) What priors could the regression model learn from, and how could it better use them? (c) How to train with noisy labels in uncertainty?

Some of the latest approaches [33, 56] design two-stage schemes to generate pseudo labels to train a regression-based model. The introduction of the pseudo-label learning framework boosts performance significantly. Unlike previous WTAL methods [8, 13, 14, 27], the key to these methods is to improve the quality of pseudo labels with post-processing strategies. However, current approaches face several limitations: they often fail to fully leverage the priors generated in the first stage, leading to suboptimal use of valuable contextual information. Furthermore, they lack effective integration with existing fully-supervised TAL frameworks, which can hinder the adaptation and consistency of the methods. We propose a two-branch (weak and full) **PseudoFormer**, focusing on addressing the following three critical problems shown in Fig. 1: (1) *How can we generate pseudo labels with confidence scores and more reliable boundaries?* (2) *How can we fully leverage the priors contained in the generated pseudo labels?* (3)

How can we effectively train a regression model with noisy pseudo labels?

To improve the quality of pseudo proposals, we introduce RickerFusion, a pseudo label generation pipeline designed to fuse outputs from a weak branch. The weak branch is functioned by a model trained using Multiple Instance Learning (MIL) [8, 14, 39]. Drawing inspiration from the Bird's Eye View (BEV) [15, 16] framework, we propose to fuse the temporal predictions from the weak branch in a shared space. Specifically, RickerFusion conceptualizes the proposal space as a top-down, unified representation where confidence scores and boundary information are treated as spatial coordinates in this space. We first follow AutoLoc [36] applying the Outer-Inner-Contrastive (OIC) score from the snippt-level predictions (SPs) to compute the proposal confidence scores. Subsequently, we map each output proposal to a Ricker wavelet [12] distribution and fuse these proposals into a unified global space. This fusion effectively consolidates predictions from diverse perspectives, allowing for noise reduction and enhanced mutual reinforcement among proposals, and ultimately capturing both the strength and spatial coherence of the detections. The fused representation is then leveraged to generate the final fused proposals. Similar to how BEV provides a global, consolidated view from multiple sources, RickerFusion can also integrate multi-scale perception into a cohesive output, improving both the accuracy and reliability of the pseudo proposals.

To effectively learn from diverse priors within pseudo labels, and bridge the gap between the frameworks between WTAL and FTAL methods, we propose a unified framework consists with a weak branch and a full branch, that learns from both video-level and proposal-level information. In the full branch, we incorporate a regression-based model, similar to mainstream TAL architectures [35, 51], to leverage the proposal-level pseudo labels generated in the weak branch. This allows the model to learn action boundaries and durations in a manner consistent with fully-supervised TAL methods. Additionally, by learning from the SPs in the weak branch, the model enriches its encoded snippt-level features with video classification information. Each pseudo label carries natural priors from the MIL process used in weak supervision, along with artificial priors introduced through design, enhancing the performance of the proposed method.

In the context of WTAL, the generated pseudo proposals are inherently noisy and lack the temporal accuracy compared to the ground-truth. To alleviate the distraction caused by wrong labels when training with noisy pseudo proposals, we introduce an uncertainty mask to enhance the robustness of our method. Recognizing that the boundaries of these proposals are likely to be less reliable compared to the centers, the mask allows us to exclude specific segments at the internal and external boundaries of each proposal from the training process. By initially focusing on the more reliable central regions, we mitigate the risk of incorporating noisy information that may distract the model. As training progresses and the model's confidence in the reliability of the proposals increases, we gradually reduce the excluded regions, eventually integrating all parts of the proposals. This adaptive approach ensures more effective training with noisy (pseudo) labels, progressively enhancing the model's ability to leverage the entire proposal information while minimizing the influence of uncertain boundary regions.

To summarize, our contribution is threefold:

- We propose PseudoFormer, a novel two-branch method for the WTAL task, which bridges the gap in both framework and performance between Weakly and Fully-supervised Temporal Action Localization.
- Considering the three primary problems, PseudoFormer utilizes the RickerFusion strategy to generate high-quality pseudo labels, leverages both video and proposal level labels with different priors, and proposes an uncertainty mask with a refinement mechanism for learning with noisy labels.
- We conduct comprehensive experiments on two benchmarks THUMOS14 [18] and ActivityNet1.3 [4]. Our method achieves significant performance over existing WTAL methods.

2. Related Work

Temporal Action Localization. Fully-supervised Temporal Action Localization (TAL) aims to simultaneously classify and localize action instances in untrimmed videos. Fully-supervised approaches can generally be categorized into two groups: two-stage methods [7, 23, 31, 45] and one-stage methods [29, 50, 54, 57]. Two-stage approaches consist of two steps: proposal generation and classification. In contrast, one-stage methods unify proposal generation and classification into a single step. Following object detection methods [5], DETR-like decoder methods are proposed [10, 25, 34, 38]. Recent advances, another series of work following ActionFormer [35, 44, 51] have led to significant performance gains. These methods build a multi-scale feature pyramid network followed by a classification and regression head. In this work, we mainly follow the mainstream actionformer-based framework.

Weakly-supervised Temporal Action Localization. To address the high cost for the snippet-level annotation, Weakly-supervised Temporal Action Localization (WTAL) has been widely studied [8, 11, 14, 26, 28, 36, 39**?**]. In contrast to fully-supervised methods, UntrimmedNet [40] was the first to adopt multi-instance learning [2, 30] for action recognition, classifying salient segments to generate action proposals without a regression head. A signif-

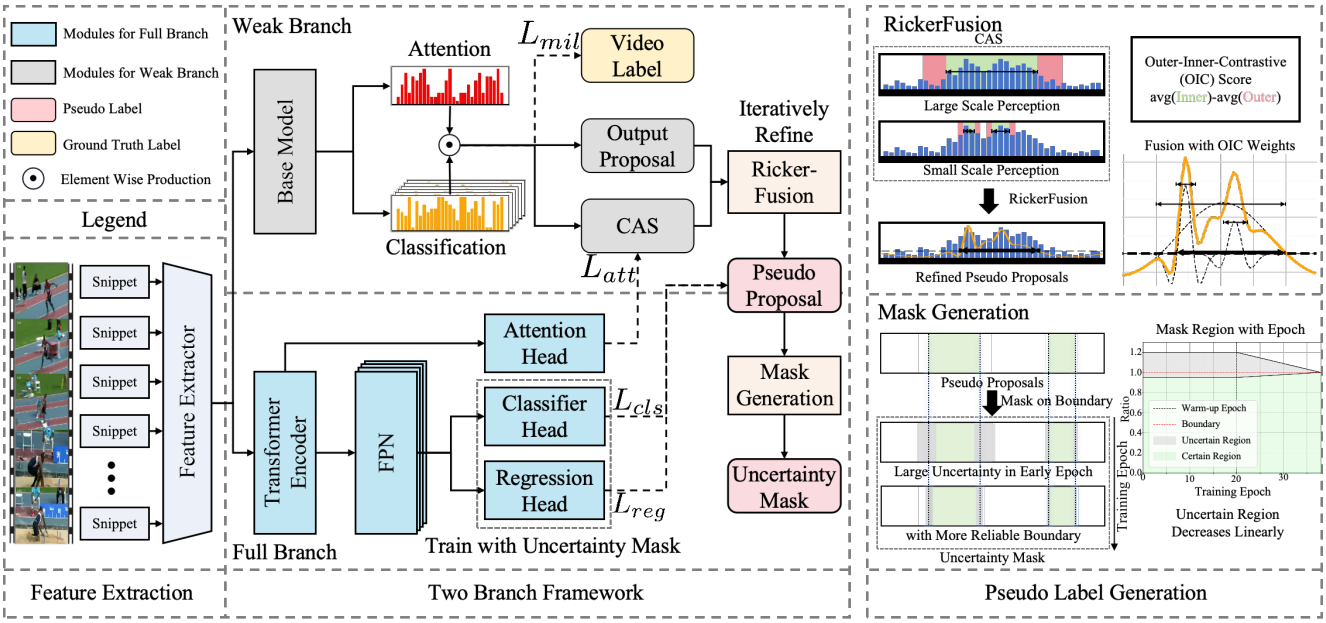

Figure 2. Overall framework of PseudoFormer. (a) **Weak Branch**: After feature extraction, the base model predicts agnostic attention and classification scores. Using Multi-instance Learning (MIL) with video-level labels, it outputs proposals and the snippt-level predictions (SPs). (b) **Full Branch**: A regression-based model is trained on the *snippt-level predictions (SPs)*, *pseudo proposals*, and *uncertainty mask*, and is used for final inference. (c) **RickerFusion**: To improve the quality of pseudo labels, RickerFusion maps predictions across perception scales into a shared space, producing better pseudo labels by fusing predictions from the weak branch. (d) **Mask Generation**: To train with noisy pseudo labels, an uncertainty mask is applied to proposal boundaries, and the uncertain regions gradually decrease after the warm-up epoch. The pseudo proposals and the uncertainty mask are iteratively refined during training.

icant body of work [8, 14, 39, 47, 48] exploits the relationship between cross-modal channels. CO2-Net [14] applies a cross-modal attention mechanism to enhance feature consistency within the structure. DDG-Net [39] directly designs a residual graph structure module to construct the cross-modal connection. A more efficient and popular method is to guide the training with uncertainty learning strategy [8, 9, 21, 46]. DELU [8] introduces evidential learning to guide the sampling strategy and learning. Recently, a line of work [1, 13, 17, 32, 33, 47] attempts to generate pseudo labels to iteratively guide the training.

Learning from Pseudo Labels. Learning from snippet-level pseudo labels could serve as a bridge between TAL and WTAL. When the example is not annotated, producing a pseudo label through confidence score thresholding is a commonly used approach in traditional methods [20, 37, 49, 53]. Between the WTAL and TAL settings, for point-supervised (PTAL) [22, 43, 52] and semi-supervised (SSTAL) [41, 42, 55] settings, several works focus on learning from the generated pseudo labels. For PTAL, based on the point annotation distribution, TSP-Net [43] proposes a center score learning method to dynamically predict the alignment from the saliency information. For SSTAL, NPL [41] iteratively generates pseudo labels with a ranking and filtering mechanism to improve the results. For WTAL, P-MIL [32] uses a two-stage framework, using pseudo labels to guide the training. Zhou et al. [56] design a Gaussian-based self-correction method to refine the boundary and score biases, thus producing pseudo labels with higher quality on the action level. PivoTAL [33] incorporates prior knowledge to generate informative proposals for regression models to learn. However, how to generate pseudo labels with better quality, how to make full use of different priors, and how to train with the noisy pseudo labels with uncertainty, still remain to be explored.

3. Method

In the Weakly-supervised Temporal Action Localization (WTAL) task, only video-level labels are provided, noted as $\mathbf{V} = \{\boldsymbol{v}_i, \boldsymbol{y}_i\}_{i=1}^{S}$, where S denotes the total number of video samples, $\boldsymbol{v}_i$ represents the i-th video, and $\boldsymbol{y}_i$ indicates the corresponding video-level category label among C categories. As shown in Fig. 2, PseudoFormer is a two-branch framework composed of a Multiple Instance Learning (MIL)-based weak branch and a regression-based full branch. The weak branch employs MIL to train a base model, generating several useful priors: the snippt-level predictions (SPs) $\boldsymbol{Z}$ and proposal set P. Through the RickerFusion and Mask Generation Modules, refined pseudo proposals $\hat{P}$ and an uncertainty mask $\boldsymbol{U}$ are produced, en-

hancing proposal quality. In the full branch, a regression-based model is trained using SPs $\boldsymbol{Z}$, the uncertainty mask $\boldsymbol{U}$, and pseudo proposals $\hat{P}$. After training, only the full-branch part is used for inference.

3.1. Weak Branch

Base Model. Following previous methods [32, 40][ref], we use off-the-shelf RGB and optical flow snippet-level features as input, denoted as $\boldsymbol{F} \in \mathbb{R}^{T\times D}$, where T denotes the number of snippets. Given the snippet-level features, a category-agnostic attention branch $\mathcal{M}^a$ is used to compute the snippt-level attention predictions (SAPs) $\boldsymbol{\varphi} \in \mathbb{R}^{T\times 1}$, and a classification branch is used to predict the snippt-level category predictions (SCPs) $\boldsymbol{\Psi} \in \mathbb{R}^{T\times(C+1)}$, where $C+1$ denotes the number of categories plus one background class.

After that, based on the assumption that background is present in all videos but filtered out by the SAPs $\boldsymbol{\varphi}$, the original predicted video-level classification scores $\hat{\boldsymbol{y}}_{base} \in \mathbb{R}^{C+1}$, and the foreground video-level classification scores $\hat{\boldsymbol{y}}_{supp} \in \mathbb{R}^{C+1}$ suppressed by attention, are derived by applying a temporal top-k aggregation strategy f_{agg} [30, 40], respectively:

$$\hat{\boldsymbol{y}}_{base} = f_{agg}(\boldsymbol{\Psi}),\ \hat{\boldsymbol{y}}_{supp} = f_{agg}(\boldsymbol{\varphi} \odot \boldsymbol{\Psi}), \tag{1}$$

where $\odot(\cdot)$ is the element-wise product.

To consider background information of each video, we extend the video-level label: $\boldsymbol{y}_{base} = [\boldsymbol{y}, 1] \in \mathbb{R}^{C+1}$ and $\boldsymbol{y}_{supp} = [\boldsymbol{y}, 0] \in \mathbb{R}^{C+1}$. Guided by the video-level category label $\boldsymbol{y} \in \mathbb{R}^{C}$, the multi-instance learning classification loss is defined as:

$$L_{mil} = -\sum_{c=1}^{C+1}(\boldsymbol{y}_{base}\log\hat{\boldsymbol{y}}_{base} + \boldsymbol{y}_{supp}\log\hat{\boldsymbol{y}}_{supp}), \tag{2}$$

Generating Different Priors. After training, the predicted snippt-level predictions (SPs), $\boldsymbol{Z} \in \mathbb{R}^{T\times(C+1)}$ is computed as $\boldsymbol{\varphi}\odot\boldsymbol{\Psi}$, which is iteratively thresholded to obtain the final localization results $P = \{(s_i, e_i, o_i, c_i)\}_{i=1}^{K}$ [8]. K is the total number of output proposals, and s_i, e_i, o_i, c_i denote the start, end, confidence score, and class for each proposal P_i, respectively. Following AutoLoc [36], we compute the score for each proposal with OIC score:

$$o_i = OIC(P_i) = avg(P_i^{inner}) - avg(P_i^{outer}), \tag{3}$$

where P_i^{inner} and P_i^{outer} are the SPs values within and outside the proposal with a fixed ratio. The OIC score effectively captures the boundary characteristics of the predicted proposals and provides a reliable measure of confidence.

After soft-NMS [3], we obtain the output proposals for proposal-level annotation, and SPs $\boldsymbol{Z}$ for snippet-level annotation with different priors from the weak branch for the full branch training.

3.2. Pseudo Label Generation

RickerFusion. The output proposals P from the base model are generated individually considering only snippet scores from SPs, ignoring the overall relationship between different proposals and scales. Additionally, the proposals are heavily overlapped due to the multi-level thresholding, which fail to accurately describe boundaries for the full branch training. Inspired by Bird's Eye View (BEV) [16], RickerFusion addresses this by mapping all proposals to a unified space to get a global perception, enhancing spatial understanding and simplifying the representation. Specifically, we use the Ricker wavelet [12], which emphasizes the center of each proposal while suppressing peripheral areas, enabling effective fusion of proposals across different scales. This approach enhances temporal action localization by achieving balanced and robust multi-scale proposal alignment, as shown in Fig. 2.

For each proposal, we map it using the Ricker distribution as follows:

$$\phi_i(t) = \frac{2}{\sqrt{3\sigma_i}\pi^{\frac{1}{4}}}(1-(\frac{t-m_i}{\sigma_i})^2)e^{-\frac{(t-m_i)^2}{2\sigma_i^2}}, \tag{4}$$

where $\sigma_i = \frac{e_i - s_i}{2}$ denotes the length, and $m_i = \frac{s_i+e_i}{2}$ denotes the midpoint of P_i. The Ricker wavelet naturally emphasizes the central part of the proposal while applying a suppression at the boundaries. For example, $\phi_i(t)$ achieves the maximum positive value when $t = m_i$, and $\phi_i(s_i) = \phi_i(e_i) = 0$. Besides, $\phi_i(t)$ will be negative, if $t < s_i$ or $t > e_i$, indicating the locations out of the proposal are suppressed. This suppression effect initially increases away from the center before gradually tapering off, helping to reduce noise and minimize the influence of less reliable boundary regions. The characteristic aligns well with the localization results, as it ensures that each proposal captures core activity with high confidence, while the regions out of the boundaries should NOT contain the target action.

Then we fuse all proposals to a shared global space as follows:

$$\Phi^l = \sum_{i=1}^{K}\phi_i o_i \cdot \mathbb{1}(c_i = l), \tag{5}$$

where $\Phi \in \mathbb{R}^{T\times C}$ denotes the final fused wavelet. Each proposal is weighted by its confidence score o_i, and predictions with incorrect classification categories are filtered out.

We obtain the final pseudo label $\hat{P} = \{(\hat{s}_i, \hat{d}_i\, \hat{c}_i\}_{i=1}^{\hat{K}}$, from Φ with a threshold of $y = 0$ for the activated area. The pseudo proposal would have better quality and more reliable boundaries.

Mask Generation. Although the generated pseudo labels achieve reasonably high quality, a significant gap remains between these pseudo labels and the true ground truth labels. To improve training with these noisy pseudo labels, we

leverage a prior assumption about proposal accuracy: the central regions of proposals tend to be more reliable, while the boundaries are more uncertain. Based on this observation, we introduce the uncertainty mask as follows:

$$\mathcal{M}_i(t) = \begin{cases} 0, & \text{if } t \in \mathcal{I}_1 \cup \mathcal{I}_2, \\ 1, & \text{otherwise.} \end{cases}$$
$$\mathcal{I} = \begin{cases} \mathcal{I}_1 = [\hat{s}_i - \alpha(\hat{e}_i - \hat{s}_i), \hat{s}_i + \beta(\hat{e}_i - \hat{s}_i)], \\ \mathcal{I}_2 = [\hat{e}_i - \beta(\hat{e}_i - \hat{s}_i), \hat{e}_i + \alpha(\hat{e}_i - \hat{s}_i)]. \end{cases} \tag{6}$$

where $\mathcal{M} \in \mathbb{R}^T$ denotes the uncertainty mask for $\hat{P}_i$, while α and β denote the expansion and shrinking ratios, respectively. Regions around the boundaries of each proposal are considered uncertain, as the pseudo labels in these areas are expected to contain more noise compared to other regions.

Then we compute the union of all masks as follows:

$$\boldsymbol{U}(t) = \bigcup_{i=1}^{\hat{K}} \mathcal{M}_i(t), \tag{7}$$

where $\boldsymbol{U} \in \mathbb{R}^{\hat{T}}$ represents the global uncertainty mask. Note that the uncertainty mask is generated at multiple scales after assigning proposals to different FPN layers, with $\hat{T}$ representing the total number of anchors across all layers.

During warm-up epochs, the uncertainty mask is used to filter out a portion of the boundary for each proposal, preventing it from involving in the training process. This uncertainty mask is designed to adapt along with the training process: as the model's confidence in the proposal boundaries increases, the uncertain regions gradually decrease linearly. As training progresses and the accuracy of the proposal boundaries improves, the mask fades, allowing the entire proposal to be utilized for training, ultimately reducing the influence of noisy labels while enhancing overall model performance.

3.3. Full Branch

Training. We introduce the regression-based model following AFormer [51] and TriDet [35]. In the training stage, the regression-based model is designed to leverage multiple priors, including SPs $\boldsymbol{Z}$ and pseudo proposals $\hat{P}$ to enhance performance. Sharing the extracted snippets with the weak branch, we first use a transformer encoder to encode the features. Then a Feature-Pyramid-Network (FPN) is applied to further process the encoded features at multiple scales as $\hat{T}$ anchors. Then we assign all pseudo proposals from $\hat{P}$ to different scales based on their duration. A Classifier Head is applied to predict the class at each anchor as follows:

$$L_{cls} = \frac{1}{N_{pos}} \sum_{t=1}^{\hat{T}} \mathbb{1}_{c_t^l > 0 \wedge \boldsymbol{U}_t = 1} \sigma_{IoU} L_{foc}(1) + \frac{1}{N_{neg}} \sum_{t=1}^{\hat{T}} \mathbb{1}_{c_t^l = 0 \wedge \boldsymbol{U}_t = 1} L_{foc}(0), \tag{8}$$

where N_{pos} and N_{neg} denote the number of foreground and background anchors, respectively. The model is trained only with anchors in certain regions specified by $\boldsymbol{U}_t$. We use focal loss L_{foc} [24] for snippt classification, and σ_{IoU} denotes the temporal IoU between the predicted proposal and the pseudo proposal.

For each anchor, the start and end of the proposal are decoded using the Regression Head. The regression loss L_{reg} is calculated as follows:

$$L_{reg} = \frac{1}{N_{pos}} \sum_{t=1}^{\hat{T}} \mathbb{1}_{c_t^l > 0 \wedge \boldsymbol{U}_t = 1} (1 - \sigma_{IoU}), \tag{9}$$

where regression loss is applied only to positive anchors.

Also, to leverage the snippet-level priors and enhance the feature representation, we apply an Attention Head and SoftMax operation for snippet-level classification before FPN. We apply L_{att} as follows:

$$L_{att} = \frac{1}{M} \sum_{t=1}^{T} \sum_{l=1}^{C+1} \mathbb{1}_{\boldsymbol{Z}_t^l > \tau} L_{foc}(l), \tag{10}$$

where M is the total number of filtered snippets, and $\boldsymbol{Z} \in \mathbb{R}^{C+1}$. Only snippets with high confidence (above threshold τ) are classified, and those with incorrect labels are filtered with $\boldsymbol{y}$.

By combining all optimization objectives introduced above, we obtain the overall loss function:

$$L = L_{reg} + L_{cls} + \lambda L_{att}, \tag{11}$$

where λ is the balancing hyper-parameter of L_{att}. We train the full branch in a teacher-student manner, following [35, 51]. The overall loss L is applied only to the student model for parameter updates, while the teacher model is updated with an exponential moving average (EMA) after warm-up epochs.

Refinement. During the full branch training stage, refinement is applied to the pseudo proposals and uncertainty mask after the warm-up epoch. Initially, the pseudo proposals $\hat{P}$ are generated by the base model. After the warm-up, the proposals produced by the regression-based model are considered to have more reliable boundaries and confidence scores.

In each training iteration, the proposal outputs from the regression model are combined with the original pseudo

Supervision	Methods	mAP@IoU(%)							AVG		
		0.1	0.2	0.3	0.4	0.5	0.6	0.7	(0.1:0.5)	(0.3:0.7)	(0.1:0.7)
Fully (TAL)	A2Net TIP'20	61.6	60.2	58.6	54.1	45.5	32.5	17.2	55.9	41.6	47.1
	Tad-MR ECCV'20	-	-	53.9	50.7	45.4	38.0	28.5	-	43.3	-
	TadTR TIP'22	-	-	74.8	69.1	60.1	46.6	32.8	-	56.7	-
	AFormer ECCV'22	-	-	82.1	77.8	71.0	59.4	43.9	-	66.8	-
	TriDet CVPR'23	87.1	86.2	83.6	80.3	73.0	62.2	46.8	82.0	69.2	74.2
Weakly (WTAL)	CO2-Net MM'21	70.1	63.6	54.5	45.7	38.3	26.4	13.4	54.4	35.7	44.6
	DELU ECCV'22	71.5	66.2	56.5	47.7	40.5	27.2	15.3	56.5	37.4	46.4
	PMIL CVPR'23	71.8	67.5	58.9	49.0	40.0	27.1	15.1	57.4	38.0	47.0
	Li et al. CVPR'23	-	-	56.2	47.8	39.3	27.5	15.2	-	37.2	-
	PivoTAL CVPR'23	74.1	69.6	61.7	52.1	42.8	30.6	16.7	60.1	40.8	49.6
	DDG-Net ICCV'23	72.5	67.7	58.2	49.0	41.4	27.6	14.8	57.9	37.9	47.3
	ISSF AAAI'24	72.4	66.9	58.4	49.7	41.8	25.5	12.8	57.8	37.6	46.8
	Ours	**76.8**	**72.6**	**65.4**	**55.6**	**44.1**	**31.3**	**17.1**	**62.9**	**42.7**	**51.9**

Table 1. Comparison results with existing methods on THUMOS14 dataset. Our method achieve state-of-the-art WTAL performance with significant improvements.

proposals $\hat{P}$ and updated through RickerFusion. This updated set of proposals is then used to refine the uncertainty mask, which guides the model toward more accurate temporal boundaries. The parameters α and β in the uncertainty mask are linearly degraded as training progresses beyond the warm-up stage. This linear degradation reflects our assumption that the proposal boundaries become increasingly reliable and accurate with further training. Consequently, the model gradually relies less on the uncertainty mask and more on the refined proposals for final predictions.

Inference. After the two-stage training, we use the regression-based full branch for inference. To obtain the video-level classification results, we first apply attention predicted by the attention head to filter the top-k scores for each class, and then average them. The predicted attention score is then used to filter the video classes, retaining only those proposals within the predicted classes. Proposals with classes below a certain threshold are discarded. Finally, we apply soft-NMS [3] to these proposals to obtain the final predictions.

4. Experiment

4.1. Datasets and Metrics

Datasets. We use two commonly used datasets for our experiments: THUMOS14 [18], and ActivityNet1.3 [4]. The THUMOS14 dataset consists of 200 validation videos and 213 testing videos, spanning 20 categories, with each video containing an average of 15.4 action instances. ActivityNet1.3 contains 10,024 training and 4,926 validation videos across 200 categories. On average, each video contains 1.6 action instances and about 36% frames are ambiguous action contexts or non-action backgrounds.

Metrics. We evaluate the TAL performance with mean Average Precision (mAP) at different Intersections over Union (IoU) thresholds. The IoU thresholds for THUMOS14 are set at [0.1:0.1:0.7], and for ActivityNet1.3 at [0.5:0.05:0.95]. Also, we present results for THUMOS14 at [0.1:0.1:0.5] and [0.3:0.1:0.7].

Implementation Details. we use DELU [8], DDG-Net [39] and CO2-Net [14] as the base model. And we follow AFormer [51] and TriDet [35] to build the regression model. To extract both RGB and optical flow features, we use Kinetics [19] pre-trained I3D [6]. The extracted features have a dimension of 1024 for both streams. For the THUMOS14 datasets, following AFormer [51], we extract one snippet feature for every 16 frames with a stride 4 (stride 16 for the base model), and for ActivityNet1.3, we extract one snippet feature for every 16 frames, with a video frame rate of 25 fps. We set the total number of epochs to 38 for THUMOS14 and 16 for ActivityNet1.3, with warm-up epochs of 20 and 10, respectively. For FPN, we use 6 layers, and we set τ to 0.8 and λ to 0.2 for L_{att}. The learning rates for THUMOS14 and ActivityNet1.3 are 1e-4 and 1e-3, respectively. For the uncertainty mask, we set $\alpha = 0.1$ and $\beta = 0$ for THUMOS14, and $\alpha = 0.05$ and $\beta = 0.05$ for ActivityNet1.3. We conduct our experiments on a single NVIDIA A40 GPU.

[1]The reported results use the same hyperparameters as those from ActivityNet1.2 in the original papers.

Supervision	Methods	mAP@IoU(%)			AVG
		0.5	0.75	0.95	(0.5:0.95)
Fully (TAL)	A2Net TIP'20	43.6	28.7	3.7	27.8
	ReAct ECCV'22	49.6	33.0	8.6	32.6
	AFormer ECCV'22	54.7	37.8	8.4	36.6
	TriDet CVPR'23	54.7	38.0	8.4	36.8
Weakly (WTAL)	CO2-Net[1] MM'21	40.8	25.6	5.7	25.6
	DELU[1] ECCV'22	40.8	26.1	6.0	25.8
	PMIL CVPR'23	41.8	25.4	5.2	25.5
	Li et al. CVPR'23	41.8	26.0	6.0	26.0
	PivoTAL CVPR'23	45.1	28.2	5.0	28.1
	DDG-Net[1] ICCV'23	40.6	26.0	6.1	25.7
	ISSF AAAI'24	39.4	25.8	6.4	25.8
	Ours	**46.9**	**28.6**	**6.5**	**29.0**

Table 2. Comparison results with existing methods on ActivityNet1.3 dataset. Our method also achieve state-of-the-art WTAL performance.

Exp	Regression Model	Ricker Fusion	Attention Loss	Uncertainty Mask	Label Refinement	AVG (0.1:0.7)
1	✗	✗	✗	✗	✗	46.4
2	✓	✗	✗	✗	✗	48.2
3	✓	✓	✗	✗	✗	50.8
4	✓	✓	✓	✗	✗	51.3
5	✓	✓	✓	✓	✗	51.6
6	✓	✓	✓	✓	✓	51.9

Table 3. Ablation study on each component of PseudoFormer.

Methods	mAP@IoU(%)							AVG
	0.1	0.2	0.3	0.4	0.5	0.6	0.7	(0.1:0.7)
Hard	72.1	66.7	58.2	48.0	36.4	25.9	14.7	46.0
Soft	75.9	70.2	61.8	50.9	38.7	25.6	14.6	48.2
Top-K	75.5	69.7	60.9	50.0	38.1	26.4	15.2	47.3
Threshold	75.0	69.9	61.4	51.6	40.6	28.1	16.3	49.0
Gauss	75.4	70.1	61.6	51.0	40.1	27.6	15.8	49.2
RickerFusion	**76.3**	**71.8**	**63.6**	**53.8**	**42.5**	**29.7**	**16.5**	**50.8**

Table 4. Comparison results between different pseudo label generation strategies with RickerFusion.

4.2. Comparison with State-of-the-art Methods

In this section, we choose DELU [8] as our base model, which is a simple yet effective baseline. Experiments with different baselines will be discussed in our ablation studies. We compare the performance of PseudoFormer with existing state-of-the-art methods on the THUMOS14 dataset in Tab. 1. We also report results from previous representative fully supervised TAL methods for reference.

We observe that PseudoFormer outperforms the base model DELU by 5.5% for average mAP at (0.1:0.7). Similar improvements are observed for other mAP scores. Compared with the previous SOTA method PivoTAL [33], which is also a 2-stage regression-based method, PseudoFormer outperforms it at each IoU threshold ranging from 0.1 to 0.7 by a large margin. The results of PseudoFormer even outperform early fully supervised TAL methods, marking a significant step towards bridging the gap between WTAL to TAL. Noting that PseudoFormer can even outperform previous fully supervised method, bridging the gap between WTAL and TAL.

We also compare PseudoFormer with existing methods on the AcitivityNet-v1.3 dataset in Tab. 2 and observe a similar trend where PseudoFormer outperforms the existing best method PivoTAL by 0.9%. In summary, our PseudoFormer achieves SOTA WTAL performance on both THUMOS14 and AcitivityNet-v1.3 benchmarks.

4.3. Ablation Study

Effectiveness of the Components. In this section, We perform ablation studies of different components in Tab. 3. As shown in Exp 1, the base model proposal achieves an average mAP of 46.4%. When directly applying all output proposals (for a snippet within several overlapping proposals, assigning the one with the highest score, details in Sec. 4.3), there is a 1.8% improvement. Using RickerFusion to improve the quality of the pseudo labels results in another significant 2.6% improvement in Exp 2. The two experiments demonstrate the effectiveness of the full branch framework and the significance of the quality of pseudo labels for performance. Introducing the attention loss in Exp 3 L_{att} enables PseudoFormer to leverage snippet-level priors, contributing an additional 0.5% improvement. This loss function enhances video-level classification and aids in optimizing encoder features before the feature pyramid network (FPN). For handling noisy labels, in Exp 4&5 the uncertainty mask yields a 0.3% gain, while label refinement provides a further 0.3% boost. These two modules help the model gradually update with better pseudo labels throughout the training process. With all modules integrated in Exp 6, PseudoFormer achieves a final performance of 51.9%, setting a new state-of-the-art.

Different Fusion Methods. As shown in Sec. 4.3, we observe that the primary improvement comes with RickerFusion. This demonstrates that the quality of the pseudo proposals is crucial for the final performance. We compare RickerFusion with different fusion methods. As shown in Tab. 4, we conduct different fusion methods to improve the quality of output proposals from the base model after soft-NMS. (1) *Hard*: For each snippet, assign it to only one proposal or background, filtering redundant overlapping proposals based on confidence scores. (2) *Soft*: Keep all proposals as input. If a snippet belongs to multiple overlapping proposals, assign it to the one with the highest confidence score. This strategy serves as the baseline in Sec. 4.3. (3) *Top-K*: For each video, select the top-K proposals with the highest confidence scores. (4) *Threshold*:

Methods	mAP@IoU(%)							AVG
	0.1	0.2	0.3	0.4	0.5	0.6	0.7	(0.1:0.7)
CO2-Net	70.1	63.6	54.5	45.7	38.3	26.4	13.4	44.6
+ PseudoFormer	**76.6**	**71.6**	**64.6**	**55.1**	**43.5**	**31.1**	**16.9**	$\mathbf{51.2}_{\uparrow 6.6}$
DELU	71.5	66.2	56.5	47.7	40.5	27.2	15.3	46.4
+ PseudoFormer	**76.8**	**72.6**	**65.4**	**55.6**	**44.1**	**31.3**	**17.1**	$\mathbf{51.9}_{\uparrow 5.5}$
DDG-Net	72.5	67.7	58.2	49.0	41.4	27.6	14.8	47.3
+ PseudoFormer	**77.2**	**72.2**	**65.8**	**56.8**	**44.8**	**31.0**	**18.4**	$\mathbf{52.4}_{\uparrow 5.1}$

Table 5. Results of PseudoFormer into different multiple instance learning base methods on THUMOS14 dataset.

Filter proposals directly based on a confidence threshold. (5) *Gauss*: Following [56], assume proposal boundaries and confidence scores follow a Gaussian distribution. We group proposals by IoU with the top proposal and compute the expected boundaries using the scores.

From Tab. 4, We observe that RickerFusion achieves the best performance. Unlike the Hard, Soft, Top-K, and Threshold strategies, RickerFusion has a light reliance on hyper-parameters. For the Gaussian strategy, pre-setting the number of proposal groups based on IoU can lead to either over-segmentation or the omission of important proposals, which reduces the overall accuracy of the full branch model. The RickerFusion emphases the centers of the proposals, while suppresses the regions out of the boundaries, achieving the best results.

Different Base Models. The proposed method focuses on utilizing generated information from the base model and effective training strategies, which are agnostic to the structure of the base locator. Consequently, PseudoFormer can be easily integrated into any Multiple Instance Learning (MIL) based WTAL method. To evaluate the generalization capability of PseudoFormer across different baselines, we employ our approach on three WTAL methods: CO2-Net [14], DELU [8], and DDG-Net [39]. The results in Tab. 5 demonstrate significant performance improvements of 6.6%, 5.5%, and 5.1% for the 3 base models when integrated with PseudoFormer. With a weaker baseline (44.6 vs 46.4), our method can still achieve similar final performance (51.2 vs 51.9). This indicates that the pseudo label generation and training pipeline is the key of our performance gain. Besides, we observe that our approach exhibits remarkable results for a strong base model DDG-Net and surpasses the current SOTA PivoTAL [33] by 2.8%. This demonstrates the generalizability of our approach.

4.4. Qualitative Analysis

We visualize some predicted action proposals in a THUMOS14 test video along the temporal axis in Fig. 3, and compare the result with the base model DELU [8]. Additionally, We visualize the pseudo labels to train the regression model after RickerFusion. For the base model, the output proposals are relatively inaccurate and scattered. The base model's multi-scale thresholding in post-processing the classification attention sequence (CAS) results in imprecise boundaries. In contrast, PseudoFormer, as a regression-based method, produces the output proposals with more accurate and consistent boundaries. The regression-based model does not rely on artificial post-processing. As shown in Fig. 3, RickerFusion enhances proposal quality from the base model, eliminates noise, and ensures each snippet belongs to one proposal or background, improving the quality of pseudo proposals.

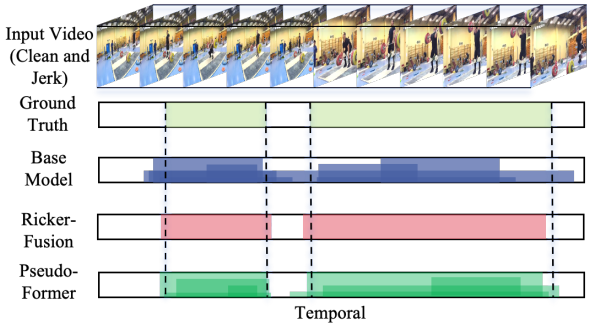

Figure 3. Visualization for ground truth on a test video, base model (DELU), after RickerFusion and PseudoFormer. For Base Model and PseudoFormer, we visualize the top-4 proposals overlapping the ground truth. With the input video, PseudoFormer produces more consistent and accurate predictions.

5. Conclusion

In this paper, we propose PseudoFormer, a two-branch framework that achieves strong results on both WTAL and PTAL tasks. We address the three primary challenges in bridging the gap in both framework and performance between Weakly-supervised and Fully-supervised Temporal Action Localization (TAL). Our method introduces a powerful pseudo-label generation strategy, leveraging RickerFusion to generate pseudo proposals with precise boundaries. By training both snippet-level and proposal-level labels, PseudoFormer enhances learning, capturing different priors from the base model. Additionally, the uncertainty mask and label refinement mechanisms effectively handle noisy labels, ensuring robust model training. This work establishes a foundation for future research in Temporal Action Localization, paving the way toward a unified framework adaptable to varying levels of supervision.

Acknowledgment

This work was supported by Beijing Natural Science Foundation under Grant 4244082, and National Natural Science Foundation of China under Grant 62402034. The authors would like to thank Prof. Junsong Yuan, and Dr. Yuanhao Zhai for useful discussions.

References

[1] Humam Alwassel, Alejandro Pardo, Fabian Caba Heilbron, Ali Thabet, and Bernard Ghanem. Refineloc: Iterative refinement for weakly-supervised action localization. In *WACV*, pages 3319–3328, 2021.

[2] Jaume Amores. Multiple instance classification: Review, taxonomy and comparative study. *Artificial Intelligence*, 201:81–105, 2013.

[3] Navaneeth Bodla, Bharat Singh, Rama Chellappa, and Larry S. Davis. Soft-nms – improving object detection with one line of code. In *ICCV*, pages 5561–5569, 2017.

[4] Fabian Caba Heilbron, Victor Escorcia, Bernard Ghanem, and Juan Carlos Niebles. Activitynet: A large-scale video benchmark for human activity understanding. In *CVPR*, pages 961–970, 2015.

[5] Nicolas Carion, Francisco Massa, Gabriel Synnaeve, Nicolas Usunier, Alexander Kirillov, and Sergey Zagoruyko. End-to-end object detection with transformers. In *ECCV*, pages 213–229, 2020.

[6] Joao Carreira and Andrew Zisserman. Quo vadis, action recognition? a new model and the kinetics dataset. In *CVPR*, 2017.

[7] Guo Chen, Yin-Dong Zheng, Limin Wang, and Tong Lu. Dcan: improving temporal action detection via dual context aggregation. In *AAAI*, pages 248–257, 2022.

[8] Mengyuan Chen, Junyu Gao, Shicai Yang, and Changsheng Xu. Dual-evidential learning for weakly-supervised temporal action localization. In *ECCV*, pages 192–208, 2022.

[9] Mengyuan Chen, Junyu Gao, and Changsheng Xu. Cascade evidential learning for open-world weakly-supervised temporal action localization. In *CVPR*, pages 14741–14750, 2023.

[10] Feng Cheng and Gedas Bertasius. Tallformer: Temporal action localization with a long-memory transformer. In *ECCV*, pages 503–521, 2022.

[11] Junyu Gao, Mengyuan Chen, and Changsheng Xu. Learning probabilistic presence-absence evidence for weakly-supervised audio-visual event perception. *IEEE Transactions on Pattern Analysis and Machine Intelligence*, 2025.

[12] Afshin Gholamy and Vladik Kreinovich. Why ricker wavelets are successful in processing seismic data: Towards a theoretical explanation. In *2014 IEEE Symposium on Computational Intelligence for Engineering Solutions (CIES)*, pages 11–16, 2014.

[13] Bo He, Xitong Yang, Le Kang, Zhiyu Cheng, Xin Zhou, and Abhinav Shrivastava. Asm-loc: Action-aware segment modeling for weakly-supervised temporal action localization. In *CVPR*, pages 13925–13935, 2022.

[14] Fa-Ting Hong, Jia-Chang Feng, Dan Xu, Ying Shan, and Wei-Shi Zheng. Cross-modal consensus network for weakly supervised temporal action localization. In *ACM MM*, pages 1591–1599, 2021.

[15] Anthony Hu, Zak Murez, Nikhil Mohan, Sofía Dudas, Jeffrey Hawke, Vijay Badrinarayanan, Roberto Cipolla, and Alex Kendall. Fiery: Future instance prediction in bird's-eye view from surround monocular cameras. In *ICCV*, pages 15273–15282, 2021.

[16] Junjie Huang, Guan Huang, Zheng Zhu, Yun Ye, and Dalong Du. Bevdet: High-performance multi-camera 3d object detection in bird-eye-view. *arXiv preprint arXiv:2112.11790*, 2022.

[17] Linjiang Huang, Liang Wang, and Hongsheng Li. Weakly supervised temporal action localization via representative snippet knowledge propagation. In *CVPR*, pages 3272–3281, 2022.

[18] Haroon Idrees, Amir R Zamir, Yu-Gang Jiang, Alex Gorban, Ivan Laptev, Rahul Sukthankar, and Mubarak Shah. The thumos challenge on action recognition for videos "in the wild". *Computer Vision and Image Understanding*, 155:1–23, 2017.

[19] Will Kay, Joao Carreira, Karen Simonyan, Brian Zhang, Chloe Hillier, Sudheendra Vijayanarasimhan, Fabio Viola, Tim Green, Trevor Back, Paul Natsev, et al. The kinetics human action video dataset. *arXiv preprint arXiv:1705.06950*, 2017.

[20] Dong-Hyun Lee et al. Pseudo-label: The simple and efficient semi-supervised learning method for deep neural networks. In *Workshop on challenges in representation learning, ICML*, page 896, 2013.

[21] Pilhyeon Lee, Jinglu Wang, Yan Lu, and Hyeran Byun. Weakly-supervised temporal action localization by uncertainty modeling. In *AAAI*, pages 1854–1862, 2021.

[22] Ping Li, Jiachen Cao, and Xingchao Ye. Prototype contrastive learning for point-supervised temporal action detection. *Expert Systems with Applications*, 213:118965, 2023.

[23] Chuming Lin, Chengming Xu, Donghao Luo, Yabiao Wang, Ying Tai, Chengjie Wang, Jilin Li, Feiyue Huang, and Yanwei Fu. Learning salient boundary feature for anchor-free temporal action localization. In *CVPR*, pages 3320–3329, 2021.

[24] Tsung-Yi Lin, Priya Goyal, Ross Girshick, Kaiming He, and Piotr Dollar. Focal loss for dense object detection. In *ICCV*, pages 2980–2988, 2017.

[25] Xiaolong Liu, Qimeng Wang, Yao Hu, Xu Tang, Shiwei Zhang, Song Bai, and Xiang Bai. End-to-end temporal action detection with transformer. *IEEE Transactions on Image Processing*, 31:5427–5441, 2022.

[26] Yangcen Liu, Ziyi Liu, Yuanhao Zhai, Wen Li, David Doerman, and Junsong Yuan. Stat: Towards generalizable temporal action localization. *arXiv preprint arXiv:2404.13311*, 2024.

[27] Ziyi Liu, Le Wang, Qilin Zhang, Wei Tang, Junsong Yuan, Nanning Zheng, and Gang Hua. Acsnet: Action-context separation network for weakly supervised temporal action localization. In *AAAI*, pages 2233–2241, 2021.

[28] Ziyi Liu, Le Wang, Qilin Zhang, Wei Tang, Nanning Zheng, and Gang Hua. Weakly supervised temporal action localization through contrast based evaluation networks. *IEEE Transactions on Pattern Analysis and Machine Intelligence*, 44(9):5886–5902, 2021.

[29] Wang Luo, Tianzhu Zhang, Wenfei Yang, Jingen Liu, Tao Mei, Feng Wu, and Yongdong Zhang. Action unit memory network for weakly supervised temporal action localization. In *CVPR*, pages 9969–9979, 2021.

[30] Oded Maron and Tomás Lozano-Pérez. A framework for multiple-instance learning. In *NeurIPS*, 1997.

[31] Zhiwu Qing, Haisheng Su, Weihao Gan, Dongliang Wang, Wei Wu, Xiang Wang, Yu Qiao, Junjie Yan, Changxin Gao, and Nong Sang. Temporal context aggregation network for temporal action proposal refinement. In *CVPR*, pages 485–494, 2021.

[32] Huan Ren, Wenfei Yang, Tianzhu Zhang, and Yongdong Zhang. Proposal-based multiple instance learning for weakly-supervised temporal action localization. In *CVPR*, pages 2394–2404, 2023.

[33] Mamshad Nayeem Rizve, Gaurav Mittal, Ye Yu, Matthew Hall, Sandra Sajeev, Mubarak Shah, and Mei Chen. Pivotal: Prior-driven supervision for weakly-supervised temporal action localization. In *CVPR*, pages 22992–23002, 2023.

[34] Dingfeng Shi, Yujie Zhong, Qiong Cao, Jing Zhang, Lin Ma, Jia Li, and Dacheng Tao. React: Temporal action detection with relational queries. In *ECCV*, pages 105–121, 2022.

[35] Dingfeng Shi, Yujie Zhong, Qiong Cao, Lin Ma, Jia Li, and Dacheng Tao. Tridet: Temporal action detection with relative boundary modeling. In *CVPR*, pages 18857–18866, 2023.

[36] Zheng Shou, Hang Gao, Lei Zhang, Kazuyuki Miyazawa, and Shih-Fu Chang. Autoloc: Weakly-supervised temporal action localization in untrimmed videos. In *ECCV*, pages 154–171, 2018.

[37] Kihyuk Sohn, David Berthelot, Nicholas Carlini, Zizhao Zhang, Han Zhang, Colin A Raffel, Ekin Dogus Cubuk, Alexey Kurakin, and Chun-Liang Li. Fixmatch: Simplifying semi-supervised learning with consistency and confidence. In *NeurIPS*, pages 596–608, 2020.

[38] Jing Tan, Jiaqi Tang, Limin Wang, and Gangshan Wu. Relaxed transformer decoders for direct action proposal generation. In *ICCV*, pages 13526–13535, 2021.

[39] Xiaojun Tang, Junsong Fan, Chuanchen Luo, Zhaoxiang Zhang, Man Zhang, and Zongyuan Yang. Ddg-net: Discriminability-driven graph network for weakly-supervised temporal action localization. In *ICCV*, pages 6622–6632, 2023.

[40] Limin Wang, Yuanjun Xiong, Dahua Lin, and Luc Van Gool. Untrimmednets for weakly supervised action recognition and detection. In *CVPR*, pages 4325–4334, 2017.

[41] Kun Xia, Le Wang, Sanping Zhou, Gang Hua, and Wei Tang. Learning from noisy pseudo labels for semi-supervised temporal action localization. In *CVPR*, pages 10160–10169, 2023.

[42] Kun Xia, Le Wang, Sanping Zhou, Gang Hua, and Wei Tang. Boosting semi-supervised temporal action localization by learning from non-target classes. *arXiv preprint arXiv:2403.11189*, 2024.

[43] Ziying Xia, Jian Cheng, Siyu Liu, Yongxiang Hu, Shiguang Wang, Yijie Zhang, and Liwan Dang. Realigning confidence with temporal saliency information for point-level weakly-supervised temporal action localization. In *CVPR*, pages 18440–18450, 2024.

[44] Le Yang, Ziwei Zheng, Yizeng Han, Hao Cheng, Shiji Song, Gao Huang, and Fan Li. Dyfadet: Dynamic feature aggregation for temporal action detection. In *ECCV*, pages 305–322, 2024.

[45] Min Yang, Guo Chen, Yin-Dong Zheng, Tong Lu, and Limin Wang. Basictad: an astounding rgb-only baseline for temporal action detection. *Computer Vision and Image Understanding*, 232:103692, 2023.

[46] Wenfei Yang, Tianzhu Zhang, Yongdong Zhang, and Feng Wu. Uncertainty guided collaborative training for weakly supervised and unsupervised temporal action localization. *IEEE Transactions on Pattern Analysis and Machine Intelligence*, 45(4):5252–5267, 2022.

[47] Yuanhao Zhai, Le Wang, Wei Tang, Qilin Zhang, Junsong Yuan, and Gang Hua. Two-stream consensus network for weakly-supervised temporal action localization. In *ECCV*, pages 37–54, 2020.

[48] Yuanhao Zhai, Le Wang, Wei Tang, Qilin Zhang, Nanning Zheng, David Doermann, Junsong Yuan, and Gang Hua. Adaptive two-stream consensus network for weakly-supervised temporal action localization. *IEEE Transactions on Pattern Analysis and Machine Intelligence*, 45(4):4136–4151, 2023.

[49] Bowen Zhang, Yidong Wang, Wenxin Hou, Hao Wu, Jindong Wang, Manabu Okumura, and Takahiro Shinozaki. Flexmatch: Boosting semi-supervised learning with curriculum pseudo labeling. In *NeurIPS*, pages 18408–18419, 2021.

[50] Chengwei Zhang, Yunlu Xu, Zhanzhan Cheng, Yi Niu, Shiliang Pu, Fei Wu, and Futai Zou. Adversarial seeded sequence growing for weakly-supervised temporal action localization. In *ACM MM*, pages 738–746, 2019.

[51] Chen-Lin Zhang, Jianxin Wu, and Yin Li. Actionformer: Localizing moments of actions with transformers. In *ECCV*, pages 492–510, 2022.

[52] Huaxin Zhang, Xiang Wang, Xiaohao Xu, Zhiwu Qing, Changxin Gao, and Nong Sang. Hr-pro: Point-supervised temporal action localization via hierarchical reliability propagation. In *AAAI*, pages 7115–7123, 2024.

[53] Pingrui Zhang, Xianqiang Gao, Yuhan Wu, Kehui Liu, Dong Wang, Zhigang Wang, Bin Zhao, Yan Ding, and Xuelong Li. Moma-kitchen: A 100k+ benchmark for affordance-grounded last-mile navigation in mobile manipulation. *arXiv preprint arXiv:2503.11081*, 2025.

[54] Jia-Xing Zhong, Nannan Li, Weijie Kong, Tao Zhang, Thomas H. Li, and Ge Li. Step-by-step erasion, one-by-one collection: A weakly supervised temporal action detector. In *ACM MM*, pages 35–44, 2018.

[55] Feixiang Zhou, Bryan Williams, and Hossein Rahmani. Towards adaptive pseudo-label learning for semi-supervised temporal action localization. In *ECCV*, pages 320–338, 2024.

[56] Jingqiu Zhou, Linjiang Huang, Liang Wang, Si Liu, and Hongsheng Li. Improving weakly supervised temporal action localization by bridging train-test gap in pseudo labels. In *CVPR*, pages 23003–23012, 2023.

[57] Zixin Zhu, Le Wang, Wei Tang, Ziyi Liu, Nanning Zheng, and Gang Hua. Learning disentangled classification and localization representations for temporal action localization. In *AAAI*, pages 3644–3652, 2022.